Whitmarsh, R.B., Sawyer, D.S., Klaus, A., and Masson, D.G. (Eds.), 1996
Proceedings of the Ocean Drilling Program, Scientific Results, Vol. 149

24. ACOUSTIC PROPERTIES OF ULTRAMAFIC ROCKS FROM THE IBERIA ABYSSAL PLAIN[1]

Dennis L. Harry[2] and Mike Batzle[3]

ABSTRACT

Serpentinized ultramafic rocks and chloritized mafic rocks recovered during ODP Leg 149 from the Iberia Abyssal Plain were examined for shear-wave anisotropy by measuring the difference in traveltime of shear waves propagating with different particle displacement orientations. The rocks are thought to represent upper mantle through lower crust exhumed during the late stages of rifting. A series of measurements was taken for shear waves propagating in the horizontal direction, with particle displacement directions varying in 10° increments from 0° to 360° in the vertical plane. Shear-wave velocity in dry samples at atmospheric pressure ranges from about 1320 to 1800 m/s in serpentinized peridotite and from about 1625 to 2000 m/s in metamorphosed mafic rocks. Shear-wave anisotropy ranges from <1% to >25% and shows a systematic increase with the intensity of veining and foliation. The greatest anisotropy occurs in strongly veined samples, with little difference observed between the amount of anisotropy in strongly foliated ultramafic rocks and moderately veined ultramafic rocks. A single sample of strongly foliated mafic rock was found to be <2% anisotropic. In the anisotropic samples, the slowest velocities were measured for waves with particle displacement perpendicular to the dominant foliation or vein direction. The fastest velocities were measured in waves with particle displacement parallel to the vein or foliation orientation. No evidence was found for anisotropy resulting from preferred grain orientation within the rock matrix, although mineral grain orientation parallel to vein or foliation orientation can not be ruled out as a possible contributor to anisotropy. In samples containing both foliation and veining, both structures contribute to anisotropy. However, the relative importance of foliation and vein orientation to anisotropic properties varied with different samples, with no obvious systematic relation between the dominant fabric and macroscopic features or composition.

INTRODUCTION

Serpentinized ultramafic rocks were recovered at Ocean Drilling Program (ODP) Sites 897, 899, and 900, which are inferred to represent upper mantle material exposed at the seafloor during the latter stages of continental rifting. At all three Leg 149 sites, the ultramafic sequence shows varying degrees of foliation, discoloration, veining, and inferred fluid alteration (Sawyer, Whitmarsh, Klaus, et al., 1994). The presence of both plagioclase feldspar and spinel in some rocks suggests that these rocks last equilibrated at shallow depths (~30 km), so the deformation features must have developed during or after the latest stages of extension.

A similar sequence of ultramafic rocks was recovered on ODP Leg 103 on the Galicia margin (Boillot, Winterer, Meyer, et al., 1987). The Leg 103 rocks show clear indications of high-temperature ductile deformation, and a strong pervasive foliation. The ductile deformation and foliation were interpreted as having developed during continental rifting along an east-dipping ductile shear zone (Girardeau et al., 1988; Boillot et al., 1989; Beslier et al., 1990). The Leg 149 ultramafic rocks are somewhat different from the Leg 103 rocks in that the foliation is not pervasive over large depth intervals and there is little indication of high-temperature ductile deformation throughout most of the recovered section. Nevertheless, the foliations and low-temperature ductile deformation features present suggest a stress history similar to that of the ultramafic rocks on the Galicia Bank, in which the foliation and deformation textures developed during late-stage shearing and exhumation of the upper mantle rocks.

One important result from Leg 103 is the observation that the foliated ultramafic rocks exhibit pronounced acoustic anisotropy, with wave propagation faster in the direction parallel to the foliations (Boillot, Winterer, Meyer, et al., 1987). The anisotropy was attributed to compositional banding related to the foliations and preferred mineral-grain orientation developed during the foliation event. Thus, anisotropy on the Galicia margin may be a good indicator of the intensity and direction of simple shear deformation during continental rifting. The ultramafic rocks recovered on Leg 149 do not display the well-developed indicators of shear that were observed in the Leg 103 samples. It is possible that this is a result of less intense shear deformation on the Iberia Abyssal Plain segment of the margin, a different style of deformation on the margin, or a different uplift history of the shallow ultramafic rocks that were recovered during the two legs. The prevalence of late-stage brecciation and multistage veining and fracture filling suggests that the rocks recovered during Leg 149 have suffered a more complex postextensional strain history than the rocks on the Galicia margin. If so, the less brecciated samples from Leg 149 may be more representative of extensional deformation.

If the relation between extensional deformation and acoustic anisotropy observed on the Galicia margin is applicable to the Iberian Abyssal Plain, then it is desirable to test for a relationship between foliation and anisotropy in the Leg 149 ultramafic rocks. We selected nine samples from Sites 897, 899, and 900 to test for acoustic anisotropy. The samples from each site represent varying degrees of foliation and intensity of veining. Acoustic anisotropy was determined by measuring the traveltime of shear waves propagating in the horizontal direction, with particle displacements oriented in 10° increments between vertical and horizontal. The traveltimes were used to deduce shear-wave velocity with various particle displacement azimuths and its relationship to veining and foliation.

[1]Whitmarsh, R.B., Sawyer, D.S., Klaus, A., and Masson, D.G. (Eds.), 1996. *Proc. ODP, Sci. Results,* 149: College Station, TX (Ocean Drilling Program).
[2]Department of Geology, The University of Alabama, Box 870338, Tuscaloosa, AL 35487, U.S.A. dharry@geophys.geo.ua.edu
[3]Geophysics Department and Institute for Resource and Environmental Geosciences, Colorado School of Mines, Golden, CO 80401, U.S.A.

EXPERIMENTAL METHOD

Sample Description

The samples used in this study were taken from Sites 897, 899, and 900 (Table 1). Petrographic descriptions given in the discussion below are taken from the shipboard core descriptions (Sawyer, Whitmarsh, Klaus, et al., 1994) and visual inspection of the samples. Site 897 was the most distal site, and Site 900 the most landward site. All samples were taken from those collected for routine shipboard velocity analyses. Minicores 25 mm in diameter, oriented perpendicular to the core (horizontal to the drill hole), were taken from the selected pieces, and the ends were trimmed to form parallel faces perpendicular to the minicore axis. The cores ranged in length from 19.5 to 25.6 mm. The direction of wave propagation was along the axis of the core, and so represents horizontal wave propagation in the Earth. All velocity measurements were done on dry samples with no confining pressure.

Apparatus

The experimental apparatus is shown in Figure 1. The technique is similar to that developed by Sondergeld et al. (1990), except that we examined the arrival time of a constant phase in the waveform (i.e., the first trough or peak) rather than picking a first break. The samples were placed in a rotating clamp, with shear-wave transducers on either end of the minicore. A 400-kHz electronic pulse similar to that described by Harry and Batzle (this volume) was sent through the transducer at one end of the sample, generating an acoustic signal that was detected by the transducer at the other end of the sample. The orientation of the transducers did not vary during the experiment, so that particle displacement was always vertical. Traveltimes were recorded at 10° intervals as the samples were rotated 360°. The shear-wave velocity at each azimuth was calculated by dividing the measured traveltime by the sample length (after correcting for the time required for the pulse to travel through the transducer assembly). Thus, minimum traveltimes were recorded at azimuths corresponding to the greatest shear-wave velocity.

Acoustic anisotropy (in percent) is given by

$$100 \times (V_{max} - V_{min})/V_{mean}\,, \quad (1)$$

where V_{max} and V_{min} are the maximum and minimum velocities and V_{mean} is the mean velocity (Kern, 1993). For simple transverse anisotropy (such as might arise from a single family of preferred mineral grain orientation, foliation, or veining) the samples should display fast and slow directions oriented 90° from each other (e.g., Kern and Tubia, 1993). This appears as two cycles of a periodic wave in the velocity vs. azimuth plot. Sample inhomogeneities or inconsistent transducer coupling introduces irregularities in the appearance of the simple harmonic wave. Microcracks opening after sample recovery may also contribute to anisotropy (Christensen and Wepfer, 1989). The samples studied show no obvious signs of post-recovery macrofractures, but measurements at elevated confining pressure would be required to test for the presence and effect of microcracks. The closure of microcracks is believed to cause the increase in velocity and decrease in anisotropy with increasing pressure that are typically observed in laboratory measurements of crystalline rocks (Christensen and Wepfer, 1989).

RESULTS

Hole 897D

The results for Hole 897D are shown in Figure 2. Sample 149-897D-23R-6 (Piece 3B) was taken from an interval of the core with sparse serpentinite-filled fractures oriented approximately 30° to vertical. The sample was taken from between veins, and it has only two thin veins visible in it. The 0° azimuth is oriented parallel to the veins. The core description reports that the piece from which this sample was taken has been replaced by 98% mesh serpentinite (Sawyer, Whitmarsh, Klaus, et al., 1994). The shear velocity varies between 1535 and 1620 m/s, with a maximum anisotropy of 5%. Slow directions are oriented at azimuths of 90° and 280°, which corresponds to particle displacement perpendicular to the orientation of the veins. Velocities vary smoothly between the fast and slow directions. The direction of slow wave propagation is consistent with the lattice-preferred orientation of vein-filling serpentine in the fractures, because serpentine is anisotropic with a slow direction of wave propagation corresponding to particle displacement across the fibers (Kern, 1993). However, mesh serpentinite is also anisotropic and the mesh texture may be at least partially inherited from the primary mineralogy (Deer et al., 1978). Thus, it is not possible to determine with certainty whether the anisotropy arises from the vein orientation or from primary preferred mineral orientation. The 5% anisotropy observed in this sample can be reasonably attributed to preferred mineral orientation, which may develop anisotropy up to 15% in olivine group minerals (Christensen and Salisbury, 1979) and has been observed as high as 35% in serpentinites at high pressure (600 MPa; Kern, 1993).

Sample 149-897D-24R-1 (Piece 3C) was taken from a moderately veined interval, and it contains less primary olivine and more primary pyroxene than Sample 149-897D-23R-6 (Piece 3B). Vein density is sufficiently high that the sample contains several visible veins, oriented approximately 30° to vertical. The 0° azimuth is parallel to the veins. Shear-wave velocities in this sample range from 1478 to 1608 m/s, for an anisotropy of about 8%. Except for a narrow range of az-

Table 1. Samples used for anisotropy study.

Core, section, interval, piece no.	Density[a] (g/cm^3)	Porosity[a,b] (%)	Description
149-897D-			
23R-6, 3B	2.43	15.89	Serpentinized peridotite, few serpentine veins
24R-1, 3C	2.45	13.40	Serpentinized peridotite, moderate serpentinite veining
25R-1, 3	2.41	12.74	Serpentinized peridotite, common serpentine veining
149-899B-			
21R-2, 1B	3.05	0.00	Serpentinite clast, no visible veins
31R-1, 12C	2.48	3.85	Serpentinized peridotite, minor serpentinite veining
34R-1, 5	2.58	1.12	Serpentinized peridotite clast, mylonitic
149-900A-			
81R-1, 1	2.82	0.00	Chloritized mafic(?) rock, foliated
85R-4, 1D	2.75	0.65	Chloritized mafic rock, foliated with later calcite veining
85R-6, 8	2.91	0.00	Mafic rock, foliated with several later generations of veining

[a] Sawyer, Whitmarsh, Klaus, et al. (1994).

[b] Porosity is assumed to be 0.00 for samples in which shipboard porosity measurements were reported to be < 0 (Sawyer, Whitmarsh, Klaus, et al., 1994).

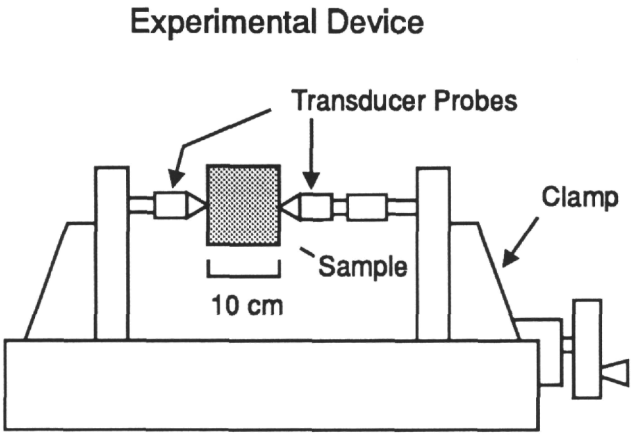

Figure 1. Illustration of the experimental apparatus. A spring-loaded clamp is used to hold the sample in a rotatable vise. Transducers at the ends of the clamping elements generate and detect the acoustic wave propagating throughout the sample. The direction of shear-wave particle displacement is vertically upward, so as the sample is rotated, shear-wave velocities with varying particle-displacement azimuths are detected.

imuths showing slow wave propagation near 100° and a narrow range of fast propagation near 260°, the velocities are fairly uniform at ~1570 m/s. The slow direction of propagation corresponds to particle displacement nearly perpendicular to the vein orientation. If the sample was transversely isotropic in the plane of wave propagation, then two slow and two fast azimuths are expected. For example, the fast azimuth should have an equally fast azimuth oriented 180° away, because this would result in identical senses of particle displacement in the sample. The lack of two fast and slow azimuths in Sample 149-897D-24R-1 (Piece 3C) suggests that the sample is not simply homogeneous and transversely isotropic, and, in fact, is typical of samples with veins cutting at oblique angles through the sample. When a shear wave impinges on a vein at an oblique angle, it is split into two waves with orthogonal particle-displacement directions (e.g., Kern, 1993), The wave with particle displacement oriented parallel to the vein is faster than the wave with particle displacement oriented perpendicular to the vein. In this sample, an obliquely oriented vein much larger than the other veins cuts the sample at an angle of about 30° to the minicore axis. We interpret the velocity data to indicate shear-wave splitting of waves striking at high angles to the orientation of this vein. The steady trend of slightly increasing velocity at azimuths between 130° and 260° indicates that the fast wave is being picked from the traveltime data, producing the narrow range of azimuths with velocities significantly different than 1570 m/s. There is no indication for significant anisotropy in the sample matrix.

Sample 149-897D-25R-1 (Piece 3) was taken from an interval showing fairly dense vertically oriented veining. The sample contains numerous veins of similar size and orientation. Like Sample 149-897D-23R-6 (Piece 3B), the primary mineralogy of this sample is mostly olivine (85%), with 15% pyroxene. The 0° azimuth is oriented parallel to the veins. This sample shows remarkably large variations in shear-wave velocity, from 1307 to 1677 m/s. Anisotropy is calculated to be 25%, with fast directions of wave propagation at 0° and 180°. This corresponds to particle displacement directions parallel to the vein orientation and is consistent with the anisotropy characteristics of fibrous vein-filling serpentinite. The shear velocity varies smoothly between the fast and slow azimuths, as is expected if the vein orientation controls the anisotropy and no single vein dominates. The anisotropy in this sample is much larger than that observed in any of the other samples studies, but is reasonable in view of the 35% anisotropy observed in serpentinite under high pressure by Kern (1993).

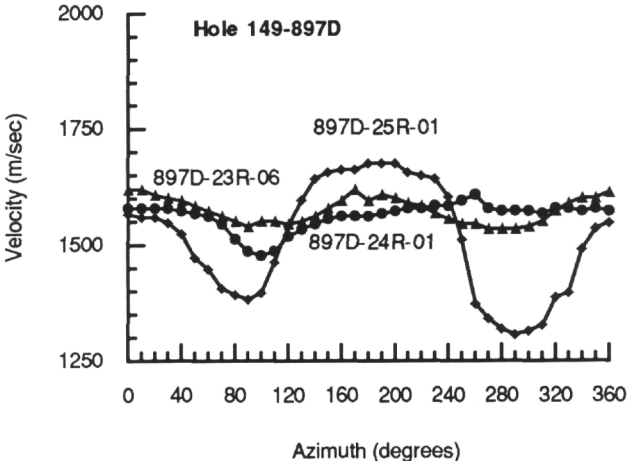

Figure 2. Calculated shear-wave velocity as a function of azimuth for samples from Hole 897D. Symbols indicate the azimuths at which velocity was measured. See text for discussion.

Hole 899B

The results for Hole 899B are shown in Figure 3. Sample 149-899B-21R-1 (Piece 1B) was taken from a pyroxene-rich clast in the Lower Breccia Unit at this site. The sample contains no significant veining. The shear-wave velocity for this sample shows little variation with azimuth, remaining close to 1590 m/s, and calculated anisotropy is less than 1%. This indicates that preferred grain-boundary orientation is absent or is insufficient to produce measurable anisotropy.

Sample 149-899B-31R-1 (Piece 12C) was taken from a nonbrecciated pyroxene-rich peridotite that has minor serpentinite veining. The 0° azimuth is oriented parallel to the veins. The sample shows a smooth variation in shear-wave velocity from 1675 to 1796 m/s, resulting in 7% anisotropy. The slowest propagation speeds are at azimuths of 90° and 280°, where particle displacement is approximately perpendicular to the dominant vein orientation.

Sample 149-899B-34R-1 (Piece 5) was taken from a piece of mylonitized peridotite, with the 0° azimuth oriented parallel to the mylonitization. The sample has unusually high shear-wave velocities at azimuths less than about 80° and greater than 320°. Arrival times at these azimuths are interpreted to come from a converted wave that is reflected off a break in the sample, which occurred during sample preparation. The break is oriented approximately 30° to the axis of the minicore and its strike is perpendicular to the 50° azimuth. The break cuts one end of the minicore approximately 3 mm from the edge. The orientation of the break is favorable for conversion of the shear wave to a compressional wave at azimuths close to 50°, producing the anomalously high velocities. Inconsistent coupling of the transducer to the sample may also be partly responsible for mode conversion, although no visual indication of coupling problems was apparent during measurement. Velocities between 80° and 320° are inferred to represent the direct shear wave. The sample shows a smooth variation in shear-wave velocity in this interval, with a maximum propagation speed at of 1690 m/s at 190° and slow propagation speeds of about 1590 m/s at 110° and 270°. This results in about 6% anisotropy, with the slow propagation direction corresponding to particle displacement perpendicular to the orientation of the mylonite fabric.

Hole 900A

The results for Hole 900A are shown in Figure 4. Sample 149-900A-81R-3 (Piece 1) was taken from a foliated breccia clast, inter-

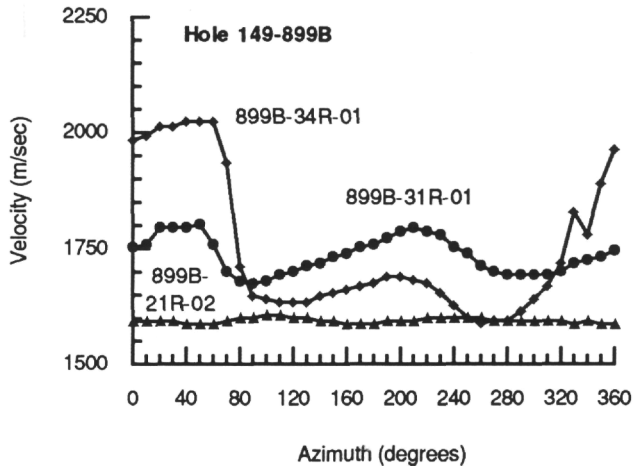

Figure 3. Calculated shear-wave velocity as a function of azimuth for samples from Hole 899B. Symbols indicate the azimuths at which velocity was measured. See text for discussion.

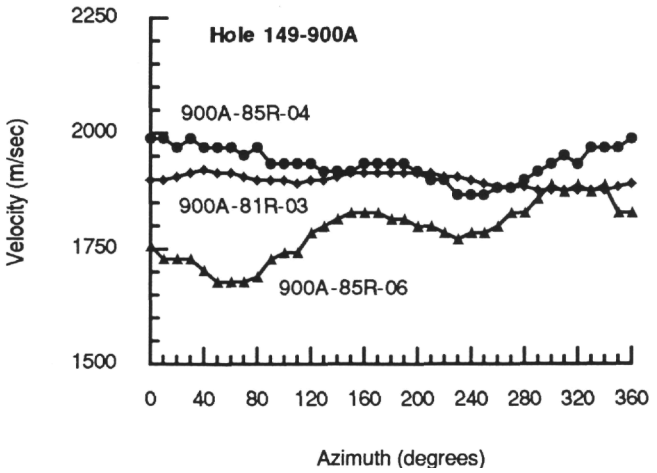

Figure 4. Calculated shear-wave velocity as a function of azimuth for samples from Hole 900A. Symbols indicate the azimuths at which velocity was measured. See text for discussion.

preted to have originally been of a mafic protolith (Sawyer, Whitmarsh, Klaus, et al., 1994). The 0° azimuth is parallel to the foliation orientation. Shipboard fabric analyses indicated that brecciation postdated the foliation, or at least continued after foliation. In spite of the well-developed foliation, this sample shows little azimuthal variation in shear-wave velocity. Anisotropy is calculated to be less than 2%, with an average shear-wave velocity of about 1900 m/s.

Sample 149-900A-85R-4 (Piece 1D) is a strongly foliated piece with a later generation of calcite veins oriented parallel to the 150° azimuth. The 0° azimuth is oriented parallel to the foliation direction. Velocity varies from 1870 to 1990 m/s, with the maximum velocity occurring at 0° azimuth, where particle displacement is parallel to the foliation. The minimum velocity occurs at 240°, where particle displacement is perpendicular to the vein orientation. An intermediate maximum velocity is measured at an azimuth of 180°, corresponding to particle displacement direction parallel to the foliation direction. The maximum anisotropy is calculated to be 6%. We infer that anisotropy arising from the foliation may be the dominant control on shear-wave propagation speed, except at azimuths where the particle displacement is nearly perpendicular to the vein orientation. The highest rate of wave propagation occurs when particle displacement is parallel to foliation. However, where the particle displacement is close to perpendicular to the vein orientation, the vein appears to dominate. The slowest propagation speeds thus occur at an azimuth perpendicular to the vein orientation.

Sample 149-900A-85R-6 (Piece 8) is a mafic rock showing some foliation and at least two generations of veining. The 0° azimuth is parallel to the foliation direction. The dark-colored, older family of veins (epidote?) reported in the core description (Sawyer, Whitmarsh, Klaus, et al., 1994) are oriented parallel to the 310° azimuth and cut the sample obliquely at an angle of about 20° to the minicore axis. A well-developed later family of epidote veins is oriented parallel to the 340° azimuth. Velocities range from 1680 to 1890 m/s, for a calculated anisotropy of 12%. As with Sample 149-900A-85R-4 (Piece 1D), the multiple vein and foliation directions result in a complicated variation of shear velocity with azimuth. In this sample, the vein orientation appears to dominate the velocity variation, because neither major nor minor maxima and minima correlate well with the foliation orientation (Fig. 4). The highest velocities are at azimuths close to the orientation of the two sets of veins (near 150° and between 300° and 340°), where particle displacement is approximately perpendicular to the veins. The second set of veins (at an azimuth of 150°) appears to best match the fastest directions of propagation.

CONCLUSIONS

The variation in shear-wave velocity with the azimuth of particle displacement (in the vertical plane) indicates that both foliation and veining contribute substantially to acoustic anisotropy in mafic and ultramafic rocks recovered from beneath the Iberia Abyssal Plain. Little evidence was found for anisotropy attributable to preferred mineral orientation in rocks that do not show significant foliation. However, it is possible that anisotropy in samples with significant veining may partially result from preferred mineral orientation parallel to the vein orientation. The vein and mineral orientations would produce identical azimuthal variations in velocity in this case. Therefore, we were not able to use the experiments to distinguish between the two if they have the same orientation. Similarly, we were unable to determine from the experiments the extent to which microcracks in the samples contribute to the observed anisotropy. Microcracks develop as a result of dilatation when the sample is decompressed during recovery. Pressure-dependent velocity changes attributed to closure of microcracks are commonly observed in crystalline rocks at pressure below about 100 MPa (Christensen and Wepfer, 1989). Because microcrack orientation may be controlled by mineral-grain orientation and/or foliation and vein fabric, it is not possible to distinguish between anisotropy arising from microcracks and anisotropy produced by structural fabric.

At Hole 897D, the amount of anisotropy observed in horizontally propagating shear waves increases in a systematic way with increasing degree of veining, from less than 5% in rocks containing only a few thin veins to 25% in strongly veined rocks. The fast direction of propagation is in directions in which particle displacement is oriented parallel to veining. At Hole 899B, anisotropy also increases systematically with the intensity of veining, ranging from less than 1 % in vein-poor clasts from the brecciated peridotite unit to 6% in rocks with minor fracturing and vein filling and in mylonitized clasts. Little difference is seen between the degree of anisotropy in mylonitized rocks and those with minor veining. At Hole 900A, the degree of anisotropy also varies systematically with the degree of foliation or veining, but seems to depend strongly on the nature of the vein material, the type of foliation, and the sequence of polyphase deformation common in the recovered rocks. A strongly foliated chloritized breccia clast (Sample 149-900A-85R-4 [Piece 10]) shows little evidence of significant anisotropy. Contrarily, a moderately foliated clast (mafic protolith) containing abundant calcite veins shows a strong anisotropy (6%). The direction of fastest wave propagation appears to be

controlled by the foliation orientation, not the vein orientation. However, rays with particle motion at a high angle to the vein orientation are substantially delayed, indicating that vein orientation may more strongly affect the propagation speed than the foliation in this narrow range of azimuths. Finally, a sample with similar intensity of foliation (Sample 149-900A-85R-6 [Piece 8]), but with two generations of epidote veins, shows a somewhat larger degree of anisotropy (12%), but in this sample the vein orientation appears to play a stronger role than the foliation in determining the propagation speed.

The samples examined in this study are a limited representation of the crystalline rocks beneath the Iberia Abyssal Plain. Furthermore, anisotropy measured at surface pressures is probably much more pronounced than anisotropy at in situ pressures (Christensen and Wepfer, 1989). Nevertheless, the experiments suggest that the structural history of the basement rocks recovered on Leg 149 can be at least partially deduced from the pattern of anisotropic wave propagation. However, the degree of anisotropy is not simply related to foliation direction or veining; it depends upon the vein composition, the polyphase deformation history of the rock, and the azimuth of particle displacement relative to foliation and vein orientation. Thus, although a careful seismic study of anisotropy beneath the Iberia Abyssal Plain may reveal information about the direction and nature of continental extension, it is important to first understand the complicated emplacement and alteration history of the rocks recovered on Leg 149 before such seismic studies can by fully understood.

ACKNOWLEDGMENTS

This research was conducted at the University of Texas at Dallas rocks physics laboratory, and at the Atlantic Richfield Company laboratories in Piano, Texas. We thank Kent Nielsen for the use of his facilities and Billy Smith for keeping the instruments running at both the UTD and ARCO labs. DLH acknowledges the support and help of Dale Sawyer in making the research logistics workable. We thank two anonymous reviewers for their helpful comments. This work was supported by USSSP grant 149-20761b to DLH.

REFERENCES

Beslier, M.-O., Girardeau, J., and Boillot, G., 1990. Kinematics of peridotite emplacement during North Atlantic continental rifting, Galicia, NW Spain. *Tectonophysics,* 184:321-343.

Boillot, G., Féraud, G., Recq, M, and Girardeau, J., 1989. "Undercrusting" by serpentinite beneath rifted margins: the example of the west Galicia margin (Spain). *Nature,* 341:523-525.

Boillot, G., Winterer, E.L., Meyer, A.W., et al., 1987. *Proc. ODP, Init. Repts.,* 103: College Station, TX (Ocean Drilling Program).

Christensen, N.I., and Salisbury, M.H., 1979. Seismic anisotropy in the oceanic upper mantle: evidence from Bay of Islands ophiolite complex. *J. Geophys. Res.,* 84:4601-4610.

Christensen, N.I., and Wepfer, W.W., 1989. Laboratory techniques for determining seismic velocities and attenuations, with applications to the continental lithosphere. *In* Pakiser, L.C., and Mooney, W.D. (Eds.), *Geophysical Framework of the Continental United States.* Mem. Geol. Soc. Am., 172:91-102.

Deer, W.A., Howie, R.A., and Zussman, J., 1978. *An Introduction to the Rock Forming Minerals:* New York (Longman).

Girardeau, J., Evans, C.A., and Beslier, M.-O., 1988. Structural analysis of plagioclase-bearing peridotites emplaced at the end of continental rifting: Hole 637A, ODP Leg 103 on the Galicia Margin. *In* Boillot, G., Winterer, E.L., et al., *Proc. ODP, Sci. Results,* 103: College Station, TX (Ocean Drilling Program), 209-223.

Kern, H., 1993. P- and S-wave anisotropy and shear-wave splitting at pressure and temperature in possible mantle rocks and their relation to the rock fabric. *Phys. Earth Planet. Inter.,* 78:245-256.

Kern, H., and Tubia, J.M., 1993. Pressure and temperature dependence of P- and S-wave velocities, seismic anisotropy and density of sheared rocks from the Sierra Alpujata massif (Ronda peridotites, southern Spain). *Earth Planet. Sci. Lett.,* 119:191-205.

Sawyer, D.S., Whitmarsh, R.B., Klaus, A., et al., 1994. *Proc. ODP, Init. Repts.,* 149: College Station, TX (Ocean Drilling Program).

Sondergeld, C.M., Rai, C.S., and Alford, R.M., 1990. Method and apparatus for detecting and measuring elastic anisotropy. U.S. Patent No. 4,912,979.

Date of initial receipt: 1 December 1994
Date of acceptance: 22 May 1995
Ms 149SR-232